

Optimization of enhanced absorption in 3D-woodpile metallic photonic crystals

Md Muntasir Hossain¹, Gengyan Chen², Baohua Jia¹, Xue-Hua Wang² and Min Gu^{1,*}

¹Centre for Micro-Photonics and CUDOS, Faculty of Engineering and Industrial Sciences,
Swinburne University of Technology, Hawthorn, Victoria 3122, Australia

²State Key Laboratory of Optoelectronic Materials and Technologies, School of Physics and Engineering,
Sun Yat-Sen University, Guangzhou 510275, China

*mgu@swin.edu.au

Abstract: We present a detailed theoretical analysis which reveals a useful insight to understand the resonant dissipative behavior of 3D woodpile metallic photonic crystals in the spectral response. We observe that a small amount of structural parameter modifications can induce great flexibility to alter the properties of the absorption resonance with even an extremely narrow band width of ~13 nm. Analyzing the dispersive properties of the 3D woodpile metallic photonic crystals and performing thorough numerical simulations for the finite number of layers we found that the magnitude, band width, and tunability of enhanced absorption can be easily optimized, which can be of significance to design an efficient photonic crystal thermal emitter.

©2010 Optical Society of America

OCIS codes: (230.5298) Photonic crystals; (160.4760) Optical properties.

References and links

1. J. G. Fleming, S.-Y. Lin, I. El-Kady, R. Biswas, and K. M. Ho, "All-metallic three-dimensional photonic crystals with a large infrared bandgap," *Nature* **417**(6884), 52–55 (2002).
2. A. Moroz, "Three-dimensional complete photonic-band-gap structures in the visible," *Phys. Rev. Lett.* **83**(25), 5274–5277 (1999).
3. I. El-Kady, M. M. Sigalas, R. Biswas, K. M. Ho, and C. M. Soukoulis, "Metallic photonic crystals at optical wavelengths," *Phys. Rev. B* **62**(23), 15299–15302 (2000).
4. C.-Y. Kuo and S.-Y. Lu, "Opaline metallic photonic crystals possessing complete photonic band gaps in optical regime," *Appl. Phys. Lett.* **92**(12), 121919 (2008).
5. T. A. Walsh, J. A. Bur, Y.-S. Kim, T.-M. Lu, and S.-Y. Lin, "High-temperature metal coating for modification of photonic band edge position," *J. Opt. Soc. Am. B* **26**(7), 1450 (2009).
6. V. Mizeikis, S. Juodkazis, R. Tarozaite, J. Juodkazyte, K. Juodkazis, and H. Misawa, "Fabrication and properties of metallo-dielectric photonic crystal structures for infrared spectral region," *Opt. Express* **15**(13), 8454–8464 (2007).
7. S. Y. Lin, J. G. Fleming, Z. Y. Li, I. El-Kady, R. Biswas, and K. M. Ho, "Origin of absorption enhancement in a tungsten, three-dimensional photonic crystal," *J. Opt. Soc. Am. B* **20**(7), 1538–1541 (2003).
8. S. Y. Lin, J. G. Fleming, and I. El-Kady, "Experimental observation of photonic-crystal emission near a photonic band edge," *Appl. Phys. Lett.* **83**(4), 593–595 (2003).
9. I. El-Kady, M. M. Sigalas, R. Biswas, K. M. Ho, and C. M. Soukoulis, "Metallic photonic crystals at optical wavelengths," *Phys. Rev. B* **62**(23), 15299–15302 (2000).
10. C. Luo, S. Johnson, J. Joannopoulos, and J. Pendry, "Negative refraction without negative index in metallic photonic crystals," *Opt. Express* **11**(7), 746–754 (2003).
11. A. Mahmoudi, A. Semnani, R. Alizadeh, and R. Adeli, "Negative refraction of a three-dimensional metallic photonic crystal," *Eur. Phys. J. Appl. Phys.* **39**(1), 27–32 (2007).
12. G. von Freymann, S. John, M. Schulz-Dobrick, E. Vekris, N. Tetreault, S. Wong, V. Kitaev, and G. A. Ozin, "Tungsten inverse opals: The influence of absorption on the photonic band structure in the visible spectral region," *Appl. Phys. Lett.* **84**(2), 224 (2004).
13. J.-H. Lee, Y.-S. Kim, K. Constant, and K.-M. Ho, "Woodpile metallic photonic crystals fabricated by using soft lithography for tailored thermal emission," *Adv. Mater.* **19**(6), 791–794 (2007).
14. Z. Y. Li, I. El-Kady, K. M. Ho, S. Y. Lin, and J. G. Fleming, "Photonic band gap effect in layer-by-layer metallic photonic crystals," *J. Appl. Phys.* **93**(1), 38–42 (2003).
15. H. Y. Sang, Z. Y. Li, and B. Y. Gu, "Engineering the structure-induced enhanced absorption in three-dimensional metallic photonic crystals," *Phys. Rev. E Stat. Nonlin. Soft Matter Phys.* **70**(6), 066611 (2004).
16. D. Sullivan, *Electromagnetic simulation using the FDTD method* (IEEE press New York, 2000).

17. A. Taflov, and S. Hagness, Computational Electrodynamics: The Finite-Difference Time-Domain Method, 3rd edn (Norwood, MA: Artech House, 2005).
18. M. S. Rill, C. Plet, M. Thiel, I. Staud, G. von Freymann, S. Linden, and M. Wegener, "Photonic metamaterials by direct laser writing and silver chemical vapour deposition," *Nat. Mater.* **7**(7), 543–546 (2008).
19. S. E. Han, A. Stein, and D. J. Norris, "Tailoring self-assembled metallic photonic crystals for modified thermal emission," *Phys. Rev. Lett.* **99**(5), 053906 (2007).
20. A. A. Krokhin, and P. Halevi, "Influence of weak dissipation on the photonic band structure of periodic composites," *Phys. Rev. B* **53**(3), 1205–1214 (1996).
21. J.-H. Lee, J. C. W. Lee, W. Leung, M. Li, K. Constant, C. T. Chan, and K.-M. Ho, "Polarization engineering of thermal radiation using metallic photonic crystals," *Adv. Mater.* **20**(17), 3244–3247 (2008).
22. M. Chen, S.-Y. Lin, H.-C. Chang, and A. S. P. Chang, "Physical origin of the resonant mode deep inside the stop band of a metallodielectric photonic crystal," *Phys. Rev. B* **78**(8), 085110 (2008).

1. Introduction

Metallic photonic crystals (MPCs) are artificial structures composed of metallic elements rather than dielectrics arranged in a periodic form. Three-dimensional (3D) MPCs are of increasing interest due to their unique electromagnetic (EM) features such as a complete and large photonic band gap [1–6], enhanced absorption of radiation [1,7], tailored thermal emission [8], beam splitters and waveguides [9], and negative refraction [10,11]. It has been realized both theoretically and experimentally that MPCs can possess enhanced absorption multiples times higher than that of the bulk material [1,7,8,12,13]. Enhanced absorptions occur in 3D MPCs at the photonic band edge and also near the resonant pass band [1,7]. This absorption region is proved to be an effective thermal radiation emission channel by suppressing the emission within the band gap and recycling the emission in the absorption region when the MPC is being heated [8]. This extraordinary potential of 3D MPCs for tailored thermal emission depends on the optimization of the band width, magnitude and tunability of the position of the absorption resonance. There have been previous studies on the optical properties of 3D woodpile MPCs with respect to the rod thickness, the number of layers and the inclusion of dielectrics [7,14,15]. However, the resonant dissipative behaviors of the 3D woodpile MPCs induced by the dispersive features and their modifications for different structural parameters are unresolved. In this work, we seek to investigate the alteration of the physical properties that induces for structural modifications by means of band structure calculations with the use of the FDTD method [16,17] and demonstrate a detailed picture of the modifications of the enhanced absorption through numerical calculations. We show that the magnitude and band width of the absorption resonance can simply be optimized and that the spectral position can widely be tuned by performing small structural modifications.

2. Band gap structures of a silver MPC

The basic formation of the MPC structure discussed here is presented in the inset of Fig. 1(a). We consider a four layer MPC consisting of rectangular metallic rods where the adjacent metallic layers are touching with one another [1]. The background of the metallic components is air. The formation of the structure is a face centered tetragonal (FCT) lattice and the stacking direction (001) is set to be the propagation direction of the incident wave. The metallic part in this MPC is considered as silver and the corresponding optical properties are defined with the classical Drude model taking the plasma frequency as $\omega_p = 1.37 \times 10^{16} \text{ s}^{-1}$ and the collision rate $\omega_c = 8.5 \times 10^{13} \text{ s}^{-1}$ [18]. The width and height of the rectangular rods are defined as w and h , respectively, and the in-layer rod spacing is d . MPCs produce a broad band gap beyond a cutoff wavelength where the transmission resonance occurs along the stacking direction, which is strongly dependent on the overall structural geometry formed by the metallic parts [7,14]. There also exists a resonant enhanced absorption peak at the photonic band edge due to the dispersive properties of the MPCs. The alteration of the metallic portion of the MPCs can greatly influence the propagation and interaction of the incident wave within the MPC environment and thus can play an effective role to properly control the anomalous enhanced absorption.

We start with numerical calculations for a silver woodpile MPC of only four layers (one unit cell) with $w = h = 300$ nm and in-layer lattice constant $a = d + w = 1\mu\text{m}$. The CST MWS studio software package is used for the calculations. The incident wave is a TE polarized (here, E parallel to the top metallic layer) plane wave through the stacking direction (001). Figure 1(a) shows the MPC possesses a wide band gap starting from wavelength $1.5\mu\text{m}$ and the first transmission resonance arises at wavelength $1.3\mu\text{m}$. We observe the noticeable enhanced absorption at the band edge near the 1st transmission peak. Almost the same result is obtained for TM polarization. These calculations are analogous to previous results reported by other studies [7,1] for a similar kind of the structural geometry, which validate our calculated results.

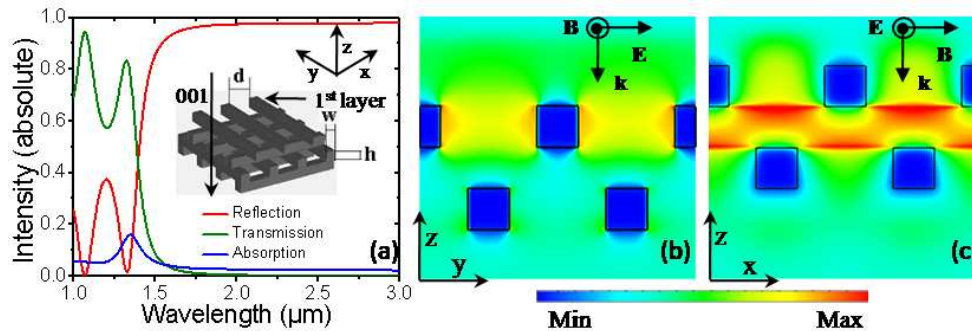


Fig. 1. (a) Calculated reflection, transmission and absorption spectra for a silver woodpile MPC with $w = h = 300$ nm, and $a = 1\mu\text{m}$. The peak absorption of the MPC occurs at wavelength $1.36\mu\text{m}$ where a high pass band exists. Inset: a schematic diagram of the silver woodpile MPC. (b) Calculated amplitude plot of the electric field inside the MPC at the band edge of wavelength $1.36\mu\text{m}$ in the y - z plane across the 2nd and 4th layers. The strong field enhancement is observed in the 2nd layer near the metallic rod surfaces. (c) Calculated amplitude plot at the band edge across the 1st and 3rd layers in the x - z plane near the metallic rod edges of the 2nd layer. Field plots are on the same scale.

This enhanced absorption is attributed to longer EM wave-matter interaction at the band edge where the EM mode is allowed but propagates with a reduced group velocity [7]. In other words these effects make the spatial decay length of the EM wave short within the MPC structure [19,20] and thus cause resonant damping (proportional to $1/V_g$) of the propagating modes. To gain the physical insight of the resonant interaction of the EM wave inside the MPC we simulate the field distribution throughout the structure. Figure 1(b) shows the amplitude plot of the electric field within the MPC in the y - z plane across the 2nd and 4th layers for the TE polarized plane waves at the band edge of wavelength $1.36\mu\text{m}$ which shows strongly enhanced field in the 2nd layer. We then take the snapshot for the TE polarized wave at the x - z plane across the 1st and 3rd layers and near the metallic surface of the 2nd layer and Fig. 1(c) clearly shows the multiple orders of the field enhanced near the edges of the metallic rods. This clearly indicates the enhanced light-matter interactions for periodicity induced slowly propagating modes near the band edge. E field enhancement was also demonstrated in two layers of periodic rectangular metallic gratings [21]. However, it should be noted that to experience a periodicity induced photonic crystal dispersive properties at the photonic band gap edge along the propagation direction at least a single unit cell [for FCT woodpile MPC four layers construct a single unit cell as shown in inset of Fig. 1(a)] of the MPC is necessary. We also notice the field enhancement occurs at the surfaces of metallic rods which are only perpendicular to the incident electric field direction. For this kind of the field distribution it was also suggested that the surface plasmon polariton propagation is not supported in such complex metallic networks. Instead the enhanced interaction of propagating light is a result of the photonic band gap effect formed by the waveguide cutoff and the coupling of the inter-layer waveguide modes [14].

To investigate the modifications of dispersive properties for different structural parameters we calculate the band diagrams of 3D silver woodpile MPCs by using Finite-Difference Time-

Domain (FDTD) method on the unit cell of woodpile structures with Bloch boundary condition [16,17]. The calculation is performed along the Γ -X (001) direction taking the $h = 0.6 \mu\text{m}$, the in-layer lattice constant $a = 1 \mu\text{m}$ and varying the w from 0.1 to $0.48 \mu\text{m}$. To calculate the eigenfrequencies of each K point in the band structure, the Bloch boundary conditions were applied to each K point. A dipole moment of a form of Gaussian pulse is placed in an appropriate position in the unit cell to excite all the eigenmodes. A monitor point within the unit cell is selected appropriately to record the time evolution of electric field $E(t)$ and the frequency spectrum of electric field $E(\omega)$ is obtained by performing Discrete Fourier Transform. The peaks in the frequency response $E(\omega)$ correspond to the eigenfrequencies. To avoid missing some eigenfrequencies whose eigenmodes accidentally have a node at or near the monitor point, we appropriately select several monitor points instead of just one monitor point, and then combine all the frequency spectrums afterwards [17]. We notice that the band structures can be divided into two kinds of band groups, the one with strong electric field amplitude $E(\omega)$ while the other with a much weaker field amplitude. The weak bands are ignored and their contribution will be discussed elsewhere. The calculated band structures are shown in Figs. 2(a)–4(d). We notice from Fig. 2(a) that for $w = 180 \text{ nm}$ the lowest energy band ends (band edge) at 136.11 THz. No allowed bands exist below that range. As the rod width w increases the band edge of the lowest band shifts to higher frequency. Also, the width of the first allowed band becomes narrower making the band flatten out which indicates the rapid change of the group velocities of the eigenmodes inside the structure. The second band gap between the 1st and 2nd allowed bands becomes wider for increasing w .

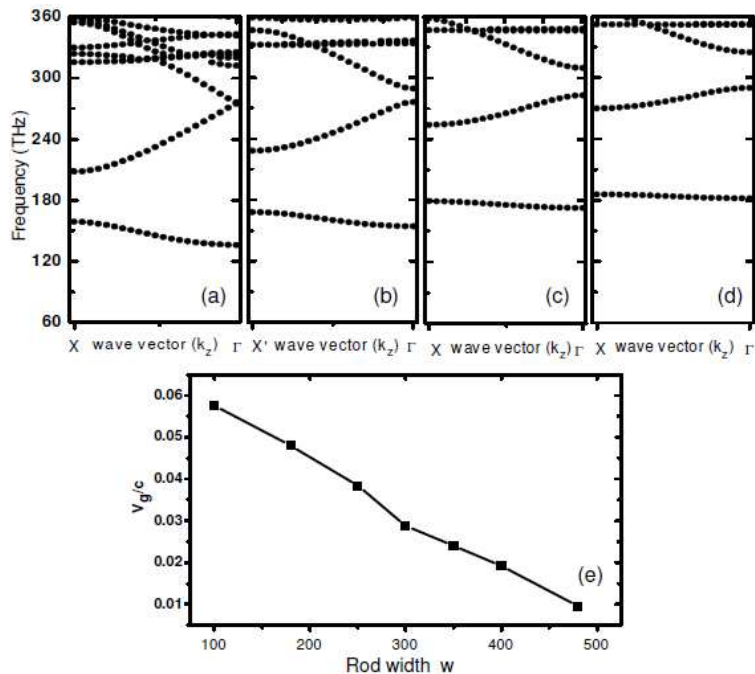


Fig. 2. (a-d) Calculated band diagrams of silver woodpile MPCs in the 001 (X- Γ) direction for $w = 0.18, 0.30, 0.42$ and $0.48 \mu\text{m}$, respectively, with a fixed rod height $h = 0.6 \mu\text{m}$. The lowest energy pass band continuously shifts to higher frequency and the band width decreases gradually for increasing w . (e) Extracted group velocity profile from the band diagrams.

To understand the physical process of the wave propagation through the MPC we extract the group velocities at the photonic band edges of the lowest energy bands for the different values of w . Figure 2(e) shows the variation of the group velocity (V_g) profile of the MPC for increasing w . V_g decreases gradually for increasing rod width. It is known that the enhanced absorption at the band edge is inversely proportional to the V_g of the EM radiation [7,19].

This suggests that in this case the absorption should increase for large w . This feature indicates that the enhanced absorption can be optimized through the alteration of the structural parameters.

3. Optimization of the enhanced absorption

For a direct comparison of the results obtained and to investigate the dependence of the resonant absorption with the group velocities we calculate the optical spectra for varying structural parameters of MPCs. Numerical calculations are performed along the 001 direction for four layers of the silver woodpile MPCs keeping the h fixed at $0.6 \mu\text{m}$. Figure 3(a) shows as we increase the filling ratio by increasing w from 0.12 to $0.30 \mu\text{m}$, the absorption spectra are found to be blue-shifted and the absorption magnitudes become strong gradually. The absorption reaches to its maximum at $w = 0.3 \mu\text{m}$ but then starts to decrease for the further increase of w . However, the group velocity profile depicted in Fig. 2(e) suggests that the absorption should gradually increase for greater w as the absorption is proportional to $1/V_g$. To understand the possible physical reason underlining this phenomenon, we look at the transmission properties of the MPCs as the absorption is nothing but the damping of the resonant eigenmodes of the pass band near the band edge.

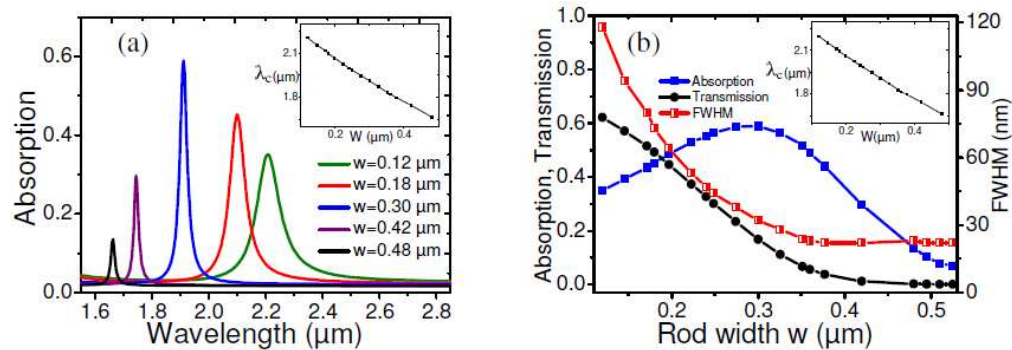


Fig. 3. (a) Calculated absolute absorption spectra for different values of w of the metallic rods in MPCs with the given value of $a = 1 \mu\text{m}$. Inset: The linear relation of the peak absorption wavelength and w . (b) Calculated absorption peaks, transmission peaks and the FWHM of the absorption as a function of w . Inset: The linear relation of the transmission peak position and w .

Figure 3(b) shows that the transmission peaks shift continuously to short wavelengths and their positions agree well with the pass bands predicted by the band diagrams depicted in Figs. 2(a)–2(d), confirming the validity of both calculations. It should be noted that the inset of Fig. 3(b) resembles the inset of Fig. 3(a) as the resonant absorption appears at the vicinity of the transmission peak. For increasing w the absorption peak completely overlaps the transmission peak position. The magnitude of the transmission falls off for increasing the filling ratios. From the band diagrams we can clearly see the widths of the lowest energy pass bands decreases for increasing w which resembles the transmissions peaks predicted by the finite numerical calculations. This suggests that for large values of w , the narrow air openings between the metallic gratings make the incident radiation difficult to penetrate and results in smaller transmission [22]. Figure 3(b) indeed shows that for increasing w the corresponding pass bands blue-shifts and their finite transmission decreases rapidly in magnitude. Thus for larger w only a small portion of the incident field can propagate with the periodicity induced extremely reduced group velocity and results in weaker absorption. It can also be noticed from Fig. 3(b) that the band widths of the absorption decrease exponentially for increasing the filling ratios, which result from the narrowing of the pass bands. Figure 3(b) shows that the full width at half maximum (FWHM) of the absorption peak for $w = 0.42 \mu\text{m}$ is 23 nm , which is more than five times smaller than the FWHM of 118 nm for $w = 0.12 \mu\text{m}$ while the peak absorptions for both do not differ too much. This feature suggests that the absorption peak position can be tuned over a broad wavelength range with a desired FWHM. As can be found

in Fig. 3(b), the absorption is the maximum (59%) at wavelength 1.91 μm for $w = 0.3 \mu\text{m}$ while the FWHM is remarkably narrow (only 32 nm).

We further investigate the magnitude, and position of the absorption spectra of MPCs with respect to the height of the metallic rods for the same values of a as that used in the previous case. We increase the height of the metallic rods gradually for a broad range from $h = 0.3 \mu\text{m}$ to $0.9 \mu\text{m}$ with taking $w = 0.3 \mu\text{m}$ in our simulations for TE waves. It can be seen from Fig. 4(a) that the absorption peaks shift to longer wavelengths for increasing h and this can be attributed to the red shift of the corresponding pass band due to the increase of the lattice constant in the propagation direction [7,14].

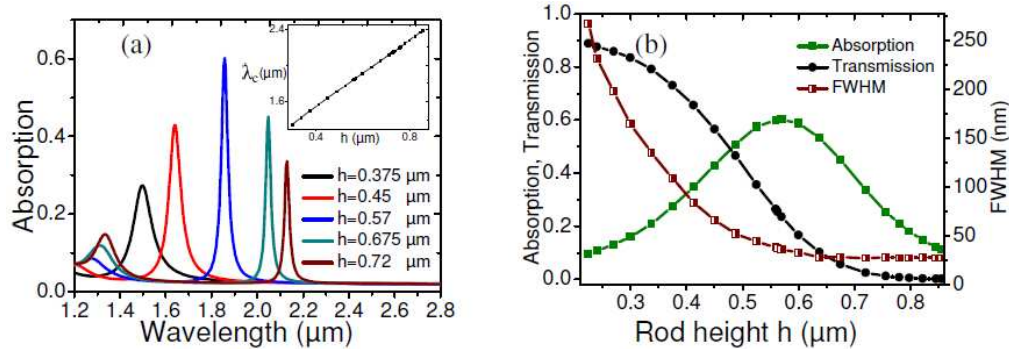


Fig. 4. (a) Calculated absorption and transmission spectra as a function of h . Inset: The linear relationship of the peak absorption wavelength and the rod thickness h . The curve follows the opposite trend to that of Fig. 3(a). (b) Calculated absorption, transmission and the FWHM of the absorption as a function of h .

The magnitude of the absorption peak increases for large h as predicted before [7]. However, for further increase of h the absorption peak reaches its maximum ($\sim 60\%$) at around $h = 0.57 \mu\text{m}$ and then surprisingly falls in magnitude keeping the red-shift as can be seen in Fig. 4(a). The decreasing value of the transmission peak for increasing h suggests that only a fraction of the incident field can propagate through the structure and results in less absorption for large value of h . The peak absorption wavelength follows a linear relation with h as can be seen in the inset of Fig. 4(a) but shows an opposite trend to that of Fig. 3(a) for varying w . The detailed spectral behavior can be seen in Fig. 4(b), which depicts that the FWHM of the absorption resonance falls exponentially for increasing h , which resembles the case in Fig. 3(b) for increasing w . The FWHM of the maximum absorption peak at $1.86 \mu\text{m}$ is only 36 nm. The transmission peak magnitude does not follow the trend of the absorption magnitude rather it gradually decreases for increasing h . An interesting feature of the considered MPC is that the transmission has a high peak value for $h < w$ (maximum 88.9% for $h = 0.225 \mu\text{m}$). This is reasonable, as the propagation length along the 001 direction effectively decreases for the small value of h , which yields less damping of the incident radiation. For MPC applications where high transmission is required such structural configuration may be useful. It is remarkable that both h and w can play a significant role to alter the resonant dissipative behavior of the woodpile MPCs. For increasing h , we also observe that the absorption peak vanishes from a finite value (only the intrinsic absorption of the metal remains) when the 1st order transmission peak completely disappears for $h > 0.9 \mu\text{m}$. The same behavior was also observed for increasing w where the absorption peak disappears for vanishing transmission resonance. These observations clearly support the argument that the enhanced absorption occurs only when there exists a pass band with finite transmission to allow the enhanced EM wave-matter interaction inside the MPC introduced by a smaller group velocity.

As the origin of the absorption resonance depends on the intrinsic absorption defined by the finite value of the imaginary part of the $\epsilon(\omega)$ [7] it is expected that the resonant spectral properties of woodpile MPCs will vary for different bulk materials. We consider a four layer MPC of gold with bulk parameters defined by the Drude model with plasma frequency $\omega_p =$

1.3647×10^{16} /s and collision rate 3.65×10^{13} /s [22]. The collision rate of the bulk gold is quite different from that of silver, which can influence the dispersive properties of the MPCs.

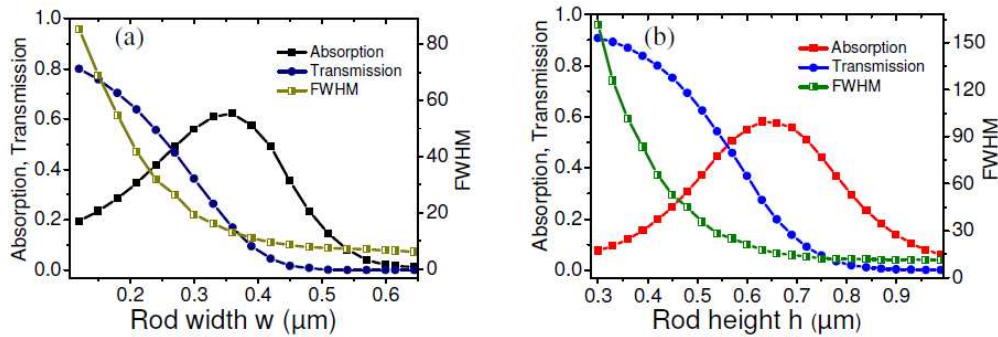


Fig. 5. (a) Calculated intensity spectra of a gold woodpile MPC for different values of w . (b) Calculated intensity spectra for different values of h . Gold MPCs show more distinctive features than silver MPCs.

We calculate the spectral properties of the gold woodpile MPCs for the same structural parameters used in the case of silver MPCs. Figures 5(a) and 5(b) show the complete optical properties of the gold MPCs for different values of w and h . Gold MPCs show even more distinctive features than that of the silver MPCs. Both Figs. 5(a) and 5(b) show the similar trends of the spectral behavior to the silver woodpile MPCs but with even narrower band widths. Figure 5(a) shows that for changing w the maximum absorption (62.2%) appears for $w = 0.36 \mu\text{m}$ at wavelength $1.82 \mu\text{m}$ with a FWHM of only 13.2 nm. This band width is more than two times narrower than the FWHM of the maximum absorption of the silver MPC for varying w . Figure 5(b) shows for increasing h the maximum absorption (58.2%) for the gold MPC appears for $h = 0.63 \mu\text{m}$ at wavelength $1.96 \mu\text{m}$ with a small value of the FWHM of 18 nm. These structural parameters and bulk material dependent resonant spectral behaviors of 3D woodpile MPCs can be very advantageous for enhanced absorption related applications.

4. Conclusion

We have theoretically investigated the resonant absorption and transmission spectra and demonstrated the inter-relation in detail for different structural conditions for 3D woodpile MPCs. We have shown that properly altering the filling ratio and the metallic rod thickness and choosing appropriate bulk material can lead to flexibly tunable absorption peak over wide spectral range with desired absorption magnitude and FWHM. As Kirchoff's law directly relates thermal emission to absorption, the potential application of MPCs for tailored thermal emission depends on the control of resonant absorption peak along with the band gap. MPCs of finite absorption magnitude with a thin band width can lead to highly efficient recycling of thermal radiation into a selected narrow emission channel.

Acknowledgement

This work was produced with the assistance of the Australian Research Council (ARC) under the Centres of Excellence program. CUDOS (the Centre for Ultrahigh-bandwidth Devices for Optical Systems) is an ARC Centre of Excellence. Baohua Jia acknowledges the ARC for the support through the APD grant DP0987006 and the ATSE for the support through the Australia China Young Scientists Exchange Program. Gengyan Chen and Xue-Hua Wang acknowledge financial support from the Chinese National Key Basic Research Special Fund, grant 2010CB923200, and the NSFC, grant 10725420.